TOPICAL REVIEW — Quantum information

Review of cavity optomechanical cooling*

Liu Yong-Chun (刘永椿)[a)†], Hu Yu-Wen (胡毓文)[a)], Wong Chee Wei (黄智维)[b)], and Xiao Yun-Feng (肖云峰)[a)‡]

[a)] *State Key Laboratory for Mesoscopic Physics and School of Physics, Peking University, Beijing* 100871, *China*
[b)] *Optical Nanostructures Laboratory, Columbia University, New York, New York* 10027, *USA*

(Received 8 October 2013; revised manuscript received 15 October 2013)

Quantum manipulation of macroscopic mechanical systems is of great interest in both fundamental physics and applications ranging from high-precision metrology to quantum information processing. For these purposes, a crucial step is to cool the mechanical system to its quantum ground state. In this review, we focus on the cavity optomechanical cooling, which exploits the cavity enhanced interaction between optical field and mechanical motion to reduce the thermal noise. Recent remarkable theoretical and experimental efforts in this field have taken a major step forward in preparing the motional quantum ground state of mesoscopic mechanical systems. This review first describes the quantum theory of cavity optomechanical cooling, including quantum noise approach and covariance approach; then, the up-to-date experimental progresses are introduced. Finally, new cooling approaches are discussed along the directions of cooling in the strong coupling regime and cooling beyond the resolved sideband limit.

Keywords: cavity optomechanics, optomechanical cooling, ground state cooling, mechanical resonator

PACS: 42.50.Wk, 07.10.Cm, 42.50.Lc **DOI:** 10.1088/1674-1056/22/11/114213

1. Introduction

Optomechanics is an emerging field exploring the interaction between light and mechanical motion. Such interaction originates from the mechanical effect of light, i.e., optical force. Radiation pressure force (or scattering force) and optical gradient force (or dipole force) are two typical categories of optical forces. The radiation pressure force originates from the fact that light carries momentum. The momentum transfer from light to a mechanical object exerts a pressure force on the object. This was noticed dating back to the 17th century by Kepler, who noted that the dust tails of comets point away from the sun. In the 1970s, Hänsch and Schawlow,[1] Wineland and Dehmelt[2] pointed out the possibility of cooling atoms by using radiation pressure force of a laser. This was subsequently realized experimentally,[3] and it has now become an important technique for manipulating atoms. The gradient force stems from the electromagnetic field gradient. The nonuniform field polarizes the mechanical object in a way that the positively and negatively charged sides of the dipole experience different forces, leading to nonzero net optical force acting on the object. It was first demonstrated by Ashkin that focused laser beams can be used to trap micro- and nano-scale particles.[4] This has stimulated the technique of optical tweezers, which are widely used to manipulate living cells, DNA, and bacteria. There are other kinds of optical forces, for instance, photothermal force (bolometric force),[5] which results from the thermalelastic effect.

The optical forces exerting on macroscopic/mesoscopic mechanical objects are typically very weak. To overcome this problem, optical cavities are employed, which resonantly enhance the intracavity light intensity so that the optical forces become pronounced. For example, in a Fabry–Pérot (FP) cavity consisting of a fixed mirror and a movable mirror attached to a spring (Fig. 1), light is reflected multiple times between the two mirrors, and thus the cavity field builds up, resulting in largely enhanced optical force exerting on the movable mirror. The study of this field named as cavity optomechanics was pioneered by Braginsky and co-workers[6,7] with microwave cavities. Later, experiments in the optical domain demonstrated the optomechanical bistability phenomenon,[8] where a macroscopic mirror had two stable equilibrium positions under the action of cavity-enhanced radiation pressure force. Further experiments observed optical feedback cooling of mechanical motion based on precise measurement and active feedback,[9,10] and along this line cooling to much lower temperatures was realized later.[11–13] On the other hand, after the observation of radiation-pressure induced self-oscillations (parametric instability) in optical microtoroidal cavities,[14–16] passive cooling, which uses purely the intrinsic backaction effect of the cavity optomechanical system, attracted much attention in the past decade.[17–27] Moreover, recent theoretical and experimental efforts have demonstrated op-

*Project supported by the National Basic Research Program of China (Grant No. 2013CB328704), the National Natural Science Foundation of China (Grant Nos. 11004003, 11222440, and 11121091), the Research Fund for the Doctoral Program of Higher Education of China (Grant No. 20120001110068), and the Scholarship Award for Excellent Doctoral Student granted by Ministry of Education, China.

†Corresponding author. E-mail: ycliu@pku.edu.cn
‡URL: www.phy.pku.edu.cn/∼yfxiao/index.html

© 2013 Chinese Physical Society and IOP Publishing Ltd

tomechanically induced transparency,[28–32] optomechanical storage,[33] normal mode splitting,[34–39] quantum-coherent coupling between optical modes and mechanical modes,[40,41] and state transfer at different optical wavelengths.[42–48] Various experimental systems are proposed and investigated, including FP cavities,[17,18] whispering-gallery microcavities,[15,49–51] microring cavities,[52] photonic crystal cavities,[53–56] membranes,[57–60] nanostrings,[61] nanorods,[62–64] hybrid plasmonic structures,[65] optically levitated particles,[66–72] cold atoms,[73–75] and superconducting circuits.[76] Recently, much attention is also focused on the studies of single-photon strong optomechanical coupling,[77–82] single-photon transport,[83–86] nonlinear quantum optomechanics,[87–90] quadratic coupling,[57,91–98] quantum superposition,[99–101] entanglement,[102–113] squeezing,[114–118] decoherence,[119] optomechanical arrays,[120,121] quantum hybrid systems,[122–126] Brillouin optomechanics,[127,128] high-precision measurements,[129–134] and so on.

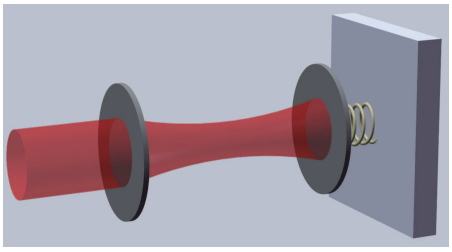


Fig. 1. Schematic of a generic optomechanical system, with a laser-driven optical cavity. The left mirror is fixed and the right mirror is movable.

The rapidly growing interest in cavity optomechanics is a result of the importance of this subject in both fundamental physics studies and applied science. On one hand, cavity optomechanics provides a unique platform for the study of fundamental quantum physics, for example, macroscopic quantum phenomena, decoherence and quantum-classical boundary. On the other hand, cavity optomechanics is promising for high-precision measurements of small forces, masses, displacements, and accelerations. Furthermore, cavity optomechanics provides many useful tools for both classical and quantum information processing. For instance, optomechanical devices can serve as storages of information, interfaces between visible light and microwave. Optomechanical systems also serve as the "bridge" or "bus" in hybrid photonic, electronic, and spintronic components, providing a routing for combining different systems to form hybrid quantum devices. A number of excellent reviews covering various topics have been published in the past.[135–157]

As the first crucial step for preparing mechanical quantum states, cooling of mechanical resonators has been one of the central research interests in the past decade. Currently, it lacks a comprehensive review on most recent theoretical and experimental progresses of cavity optomechanical cooling, especially new cooling approaches for guiding future experiments. In this review, we focus on this issue, addressing the quantum theory, recent experiments, and new directions. The rest of this paper is organized as follows. In Section 2, we present the basic quantum theory of cavity optomechanical cooling. Starting from the system Hamiltonian, we introduce the linearization of the interaction. Then, the methods for calculating the cooling rates and cooling limits are shown, including quantum noise approach and covariance approach. In Section 3, we review the up-to-date experimental progress towards cooling to the quantum ground state. Recent theoretical approaches for improving the cooling performance are discussed in Section 4. A summary is presented in Section 5.

2. Quantum theory of cavity optomechanical cooling

The basic idea of cavity optomechanical cooling is that the optical field introduces extra damping for the mechanical mode. Qualitatively, such optical damping is introduced because the optical force induced by the cavity field reacts with a finite delay time, corresponding to the photon lifetime of the cavity. Let us take a FP cavity optomechanical system as an example (Fig. 1). On one hand, when the movable mirror is at different positions, the cavity fields and thus the optical force exerting on the mirror is also different. On the other hand, when the position of the movable mirror changes, the subsequent change of the cavity field requires some time-lag due to the finite photon lifetime. Therefore, the optical force also depends on the velocity of the movable mirror. This velocity-dependent optical force is similar to the friction caused by the intrinsic mechanical damping, and leads to extra damping (or amplification) of the mechanical motion. In the classical picture, for an optical damping rate $\Gamma_{\rm opt}$, the resulting effective temperature of the mechanical mode being cooled is $T_{\rm eff} = \gamma T/(\gamma+\Gamma_{\rm opt})$, where γ is the intrinsic mechanical damping rate and T is the environmental temperature. Note that the mechanical mode is selectively cooled, i.e., only the mode of interest is cooled while the bulk temperature of the mechanical object keeps unchanged. For the FP cavity case, the mechanical mode of interest is the center-of-mass motion of the movable mirror.

The above classical description of cavity optomechanical cooling is not accurate in some cases. For example, it does not predict cooling limits.[158–160] To accurately model the cooling process, in the following, we provide full quantum theory of cavity optomechanical cooling. Here, both the cavity field and the mechanical oscillation are described as quantized bosonic fields. Starting from the system Hamiltonian and taking the dissipations into consideration, we can write down the quantum Langevin equations and master equation to describe the

system dynamics. For different parameter regimes, cooling performance can be obtained using different approaches.

2.1. System Hamiltonian and linearization

Let us consider a generic cavity optomechanical system with a single optical cavity mode coupled to a mechanical mode, which is canonically modeled as a FP cavity with one fixed mirror and one movable mirror mounted on a spring (Fig. 1). The system Hamiltonian is given by

$$H = H_{\rm free} + H_{\rm int} + H_{\rm drive}. \tag{1}$$

The first term ($H_{\rm free}$) is the free Hamiltonian of the optical and mechanical modes, described by

$$H_{\rm free} = \omega_{\rm c} a^{\dagger} a + \omega_{\rm m} b^{\dagger} b. \tag{2}$$

Here, both of the optical and the mechanical modes are represented by quantum harmonic oscillators, where a ($a^{\dagger}$) is the bosonic annihilation (creation) operator of the optical cavity mode, b ($b^{\dagger}$) is the bosonic annihilation (creation) operator of the mechanical mode, and $\omega_{\rm c}$ ($\omega_{\rm m}$) is the corresponding angular resonance frequency. The commutation relations satisfy $[a, a^{\dagger}] = 1$ and $[b, b^{\dagger}] = 1$. The displacement operator of the mechanical mode is given by $x = x_{\rm ZPF}(b^{\dagger} + b)$, where $x_{\rm ZPF} = \sqrt{\hbar/(2m_{\rm eff}\omega_{\rm m})}$ is the zero-point fluctuation, with $m_{\rm eff}$ being the effective mass of the mechanical mode.

The second term of Eq. (1) ($H_{\rm int}$) describes the optomechanical interaction between the optical mode and the mechanical mode, which is written as

$$H_{\rm int} = g a^{\dagger} a (b^{\dagger} + b), \tag{3}$$

where $g = [\partial \omega_{\rm c}(x)/\partial x] x_{\rm ZPF}$ represents the single-photon optomechanical coupling strength. This Hamiltonian can be obtained by simply considering that the cavity resonance frequency is modulated by the mechanical position and using Taylor expansion $\omega_{\rm c}(x) = \omega_{\rm c} + x\partial\omega_{\rm c}(x)/\partial x + \mathcal{O}(x) \simeq \omega_{\rm c} + g(b^{\dagger} + b)$. A more rigorous and detailed derivation of this Hamiltonian can be found in Law's paper.[161] Note that we focus on the radiation pressure force and the optical gradient force. For the photothermal force, the Hamiltonian can be found in Ref. [162].

The last term of Eq. (1) ($H_{\rm drive}$) describes the optical driving of the system. Assume that the system is excited through a coherent continuous-wave laser, and then the Hamiltonian is given by

$$H_{\rm drive} = \Omega^{*} \mathrm{e}^{\mathrm{i}\omega_{\rm in} t} a + \Omega \mathrm{e}^{-\mathrm{i}\omega_{\rm in} t} a^{\dagger}. \tag{4}$$

Here, $\omega_{\rm in}$ is the input laser frequency and $\Omega = \sqrt{\kappa_{\rm ex} P/(\hbar\omega_{\rm in})}\, \mathrm{e}^{\mathrm{i}\phi}$ denotes the driving strength, where P is the input laser power, ϕ is the initial phase of the input laser, and $\kappa_{\rm ex}$ is the input-cavity coupling rate.

In the frame rotating at the input laser frequency $\omega_{\rm in}$, the system Hamiltonian is transformed to

$$H = -\Delta a^{\dagger} a + \omega_{\rm m} b^{\dagger} b + g a^{\dagger} a (b^{\dagger} + b) + (\Omega^{*} a + \Omega a^{\dagger}), \tag{5}$$

where $\Delta = \omega_{\rm in} - \omega_{\rm c}$ is the input-cavity detuning. The quantum Langevin equations are given by

$$\begin{aligned} \dot{a} &= \left(\mathrm{i}\Delta - \frac{\kappa}{2}\right) a - \mathrm{i} g a (b + b^{\dagger}) \\ &\quad - \mathrm{i}\Omega - \sqrt{\kappa_{\rm ex}} a_{\rm in,ex} - \sqrt{\kappa_0} a_{\rm in,0}, \end{aligned} \tag{6}$$

$$\dot{b} = \left(-\mathrm{i}\omega_{\rm m} - \frac{\gamma}{2}\right) b - \mathrm{i} g a^{\dagger} a - \sqrt{\gamma} b_{\rm in}, \tag{7}$$

where κ_0 is the intrinsic cavity dissipation rate; $\kappa = \kappa_0 + \kappa_{\rm ex}$ is the total cavity dissipation rate; γ is the dissipation rate of the mechanical mode; $a_{\rm in,0}$, $a_{\rm in,ex}$, and $b_{\rm in}$ are the noise operators associated with the intrinsic cavity dissipation, external cavity dissipation (input-cavity coupling), and mechanical dissipation. The correlations for these noise operators are given by

$$\langle a_{\rm in,0}(t) a^{\dagger}_{\rm in,0}(t') \rangle = \langle a_{\rm in,ex}(t) a^{\dagger}_{\rm in,ex}(t') \rangle = \delta(t - t'), \tag{8}$$

$$\langle a^{\dagger}_{\rm in,0}(t) a_{\rm in,0}(t') \rangle = \langle a^{\dagger}_{\rm in,ex}(t) a_{\rm in,ex}(t') \rangle = 0, \tag{9}$$

$$\langle b_{\rm in}(t) b^{\dagger}_{\rm in}(t') \rangle = (n_{\rm th} + 1)\delta(t - t'), \tag{10}$$

$$\langle b^{\dagger}_{\rm in}(t) b_{\rm in}(t') \rangle = n_{\rm th}\delta(t - t'). \tag{11}$$

Here, $n_{\rm th}$ is the thermal phonon number given by

$$n_{\rm th} = \left(\mathrm{e}^{\hbar\omega_{\rm m}/k_{\rm B}T} - 1\right)^{-1}, \tag{12}$$

where T is the environmental temperature and $k_{\rm B}$ is Boltzmann constant. Note that for microwaves, the thermal occupations should also be included in Eqs. (8) and (9). Here, we focus on optical frequencies and thus the thermal photon number is negligible.

Coherent laser input results in the displacements of both the optical and mechanical harmonic oscillators. For convenience, a displacement transformation is applied, i.e., $a \to a_1 + \alpha$, $b \to b_1 + \beta$, where α and β are c numbers, denoting the displacements of the optical and mechanical modes; a_1 and b_1 are the displaced operators, representing the quantum fluctuations of the optical and mechanical modes around their classical values. By separating the classical and quantum components, the quantum Langevin equations are rewritten as

$$\dot{\alpha} = \left(\mathrm{i}\Delta' - \frac{\kappa}{2}\right) \alpha - \mathrm{i}\Omega, \tag{13}$$

$$\dot{\beta} = \left(-\mathrm{i}\omega_{\rm m} - \frac{\gamma}{2}\right) \beta - \mathrm{i} g |\alpha|^2, \tag{14}$$

$$\begin{aligned} \dot{a}_1 &= \left(\mathrm{i}\Delta' - \frac{\kappa}{2}\right) a_1 - \mathrm{i} g \alpha (b_1 + b_1^{\dagger}) - \mathrm{i} g a_1 (b_1 + b_1^{\dagger}) \\ &\quad - \sqrt{\kappa_{\rm ex}} a_{\rm in,ex} - \sqrt{\kappa_0} a_{\rm in,0}, \end{aligned} \tag{15}$$

$$\begin{aligned} \dot{b}_1 &= \left(-\mathrm{i}\omega_{\rm m} - \frac{\gamma}{2}\right) b_1 - \mathrm{i} g \left(\alpha^{*} a_1 + \alpha a_1^{\dagger}\right) \\ &\quad - \mathrm{i} g a_1^{\dagger} a_1 - \sqrt{\gamma} b_{\rm in}, \end{aligned} \tag{16}$$

where the optomechanical-coupling modified detuning $\Delta' = \Delta - g(\beta + \beta^{*})$. Under strong driving condition, the classical

components dominate and the nonlinear terms $iga_1(b_1+b_1^\dagger)$ and $iga_1^\dagger a_1$ in Eqs. (15) and (16) can be neglected, respectively. Then, we obtain the linearized quantum Langevin equations for a_1 and b_1, and the corresponding Hamiltonian is given by

$$H_L = -\Delta' a_1^\dagger a_1 + \omega_m b_1^\dagger b_1 + (Ga_1^\dagger + G^* a_1)(b_1 + b_1^\dagger), \quad (17)$$

where $G = \alpha g$ is the coherent intracavity field enhanced optomechanical coupling strength.

Initially, the phonons are in a thermal equilibrium state the thermal phonon number is n_{th}. Then, the interaction between the photons and the phonons, as described by the last term in Eq. (17), leads to the modification of the phonon number. Figure 2 displays the level diagram and the coupling routes among different states,[163] where $|n,m\rangle$ represents the number state with n (m) being the photon (phonon) number in the displaced frame. Denoted by the dashed curves, there are three kinds of heating processes: swap heating (B), quantum backaction heating (D), and thermal heating (F). Thermal heating is an incoherent process arising from the interaction between the mechanical object and the environment. Swap heating and quantum backaction heating are the accompanying effect when radiation pressure is utilized to cool the mechanical motion, corresponding to the coherent interaction processes $a_1 b_1^\dagger$ and $a_1^\dagger b_1^\dagger$, respectively. Swap heating emerges when the system is in the strong coupling regime which enables reversible energy exchange between photons and phonons. Meanwhile, quantum backaction heating can pose a fundamental limit for backaction cooling. The solid curves (A, C, and E) illustrate cooling processes associated with energy swapping, counter-rotating-wave interaction, and cavity dissipation. In the following, we derive the cooling rates and cooling limits by taking all the above processes.

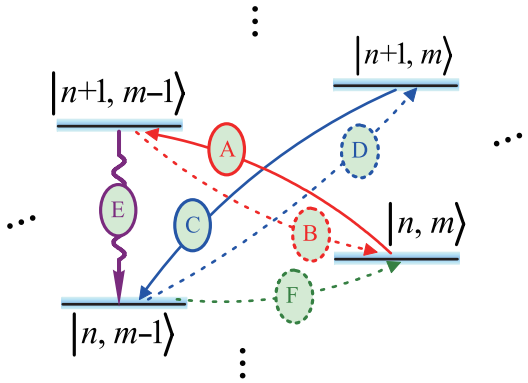


Fig. 2. Level diagram of the linearized Hamiltonian (17), the $|n,m\rangle$ denotes the state of n photons and m phonons in the displaced frame. The solid (dashed) curves with arrows correspond to the cooling (heating) processes. See text for details. Figures reproduced with permission from Ref. [163], copyright (2013) by the American Physical Society.

2.2. Quantum noise approach

In the weak coupling regime, the optomechanical cooling can be analyzed using the perturbation theory, where optomechanical coupling is regarded as a perturbation to the optical field. The power spectrum of the optical force exerting on the mechanical motion $S_{FF}(\omega)$ is calculated with the absence of coupling to the mechanical resonator. Then, the cooling (heating) rate is proportional to $S_{FF}(\pm\omega_m)$, corresponding to the ability for absorbing (emitting) a phonon by the intracavity field.

From Eq. (17), we obtain the optical force acting on the mechanical motion, described by $F = -(G^* a_1 + G a_1^\dagger)/x_{ZPF}$. The quantum noise spectrum of the optical force is given by the Fourier transformation of the autocorrelation function $S_{FF}(\omega) \equiv \int \langle F(t)F(0)\rangle e^{i\omega t} dt$. The calculation is best performed in the frequency domain. In the absence of the optomechanical coupling, from Eq. (15), we obtain

$$\begin{aligned} -i\omega\tilde{a}_1(\omega) &= \left(i\Delta' - \frac{\kappa}{2}\right)\tilde{a}_1(\omega) - \sqrt{\kappa_{ex}}\tilde{a}_{in,ex}(\omega) \\ &\quad - \sqrt{\kappa_0}\tilde{a}_{in,0}(\omega), \end{aligned} \quad (18)$$

which yields

$$\tilde{a}_1(\omega) = \frac{\sqrt{\kappa}\tilde{a}_{in}(\omega)}{i(\omega+\Delta') - \kappa/2}, \quad (19)$$

where $\tilde{a}_{in}(\omega) = \sqrt{\kappa_{ex}/\kappa}\tilde{a}_{in,ex}(\omega) + \sqrt{\kappa_0/\kappa}\tilde{a}_{in,0}(\omega)$. Using $F(\omega) = -[G^*\tilde{a}_1(\omega) + G\tilde{a}_1^\dagger(\omega)]/x_{ZPF}$, the spectral density of the optical force is obtained as

$$S_{FF}(\omega) = \frac{\kappa|G\chi(\omega)|^2}{x_{ZPF}^2} = \frac{|G|^2}{x_{ZPF}^2}\frac{\kappa}{(\omega+\Delta')^2 + \kappa^2/4}. \quad (20)$$

The rate for absorbing and emitting a phonon by the cavity field are respectively given by

$$A_\mp = S_{FF}(\pm\omega_m)x_{ZPF}^2 = \frac{|G|^2\kappa}{(\omega_m \pm \Delta')^2 + \kappa^2/4}. \quad (21)$$

We can also derive the spectral density of the mechanical mode $S_{bb}(\omega)$ by considering the full equations (Eqs. (15) and (16))

$$\begin{aligned} -i\omega\tilde{a}_1(\omega) &= \left(i\Delta' - \frac{\kappa}{2}\right)\tilde{a}_1(\omega) - iG[\tilde{b}_1^\dagger(\omega) + \tilde{b}_1(\omega)] \\ &\quad - \sqrt{\kappa_{ex}}\tilde{a}_{in,ex}(\omega) - \sqrt{\kappa_0}\tilde{a}_{in,0}(\omega), \end{aligned} \quad (22)$$

$$\begin{aligned} -i\omega\tilde{b}_1(\omega) &= \left(-i\omega_m - \frac{\gamma}{2}\right)\tilde{b}_1(\omega) - i[G^*\tilde{a}_1(\omega) \\ &\quad + G\tilde{a}_1^\dagger(\omega)] - \sqrt{\gamma}\tilde{b}_{in}(\omega), \end{aligned} \quad (23)$$

from which we obtain

$$\tilde{b}_1(\omega) \simeq \frac{\sqrt{\gamma}\tilde{b}_{in}(\omega) - i\sqrt{\kappa}\left[G^*\chi(\omega)\tilde{a}_{in}(\omega) + G\chi^*(-\omega)\tilde{a}_{in}^\dagger(\omega)\right]}{i\omega - i[\omega_m + \Sigma(\omega)] - \gamma/2}, \quad (24)$$

where

$$\Sigma(\omega) = -\mathrm{i}\,|G|^2\,[\chi(\omega) - \chi^*(-\omega)], \tag{25}$$

$$\chi(\omega) = \frac{1}{-\mathrm{i}(\omega+\Delta') + \kappa/2}. \tag{26}$$

In the second step of the derivation we have neglected the terms containing $\tilde{b}_1^\dagger(\omega)$, which is negligible near $\omega = \omega_\mathrm{m}$. Here, $\Sigma(\omega)$ represents the optomechanical self energy and $\chi(\omega)$ is the response function of the cavity mode. It shows that the optomechanical coupling leads to the modification of both the mechanical resonance frequency and the mechanical damping rate, which are termed as optical spring effect and optical damping effect, respectively. The frequency shift $\delta\omega_\mathrm{m}$ and the extra damping Γ_opt are given by

$$\begin{aligned}\delta\omega_\mathrm{m} &= \mathrm{Re}\Sigma(\omega_\mathrm{m}) \\ &= |G|^2\,\mathrm{Im}\left[\frac{1}{-\mathrm{i}(\omega_\mathrm{m}+\Delta')+\kappa/2}\right. \\ &\quad \left. - \frac{1}{-\mathrm{i}(\omega_\mathrm{m}-\Delta')+\kappa/2}\right], \end{aligned} \tag{27}$$

$$\begin{aligned}\Gamma_\mathrm{opt} &= -2\,\mathrm{Im}\Sigma(\omega_\mathrm{m}) \\ &= 2\,|G|^2\,\mathrm{Re}\left[\frac{1}{-\mathrm{i}(\omega_\mathrm{m}+\Delta')+\kappa/2}\right. \\ &\quad \left. - \frac{1}{-\mathrm{i}(\omega_\mathrm{m}-\Delta')+\kappa/2}\right]. \end{aligned} \tag{28}$$

The spectral density of the mechanical mode is given by

$$\begin{aligned}S_\mathrm{bb}(\omega) &= \int_{-\infty}^{\infty} \tilde{b}_1^\dagger(\omega)\,\tilde{b}_1(\omega')\,\mathrm{d}\omega' \\ &= \frac{\gamma n_\mathrm{th} + \kappa|G\chi(-\omega)|^2}{|\mathrm{i}\omega - \mathrm{i}(\omega_\mathrm{m} + \Sigma(\omega)) - (\gamma/2)|^2}. \end{aligned} \tag{29}$$

Figure 3 plots the normalized $S_\mathrm{FF}(\omega)$ for different laser detunings. It shows that red detuning leads to $A_- > A_+$, corresponding to cooling. In this case, typically the optical damping rate $\Gamma_\mathrm{opt} = A_- - A_+$ is much larger than the intrinsic mechanical damping rate, and then the cooling limit is obtained as

$$n_\mathrm{f} = \frac{\gamma n_\mathrm{th} + A_+}{\Gamma_\mathrm{opt}}. \tag{30}$$

Note that $n_\mathrm{f}^\mathrm{c} = \gamma n_\mathrm{th}/\Gamma_\mathrm{opt}$ is the classical cooling limit while $n_\mathrm{f}^\mathrm{q} = A_+/\Gamma_\mathrm{opt}$ corresponds to the fundamental quantum limit, as the heating rate A_+ originates from the quantum backaction. This fundamental limit can be simplified as

$$n_\mathrm{f}^\mathrm{q} = \frac{4(\omega_\mathrm{m}+\Delta')^2 + \kappa^2}{-16\omega_\mathrm{m}\Delta'}. \tag{31}$$

The minimal cooling limit is given by

$$n_\mathrm{f,min}^\mathrm{q} = \frac{1}{2}\left(\sqrt{1 + \frac{\kappa^2}{4\omega_\mathrm{m}^2}} - 1\right), \tag{32}$$

obtained when $\Delta' = -\sqrt{\omega_\mathrm{m}^2 + \kappa^2/4}$.

In particular, in the unresolved sideband regime ($\omega_\mathrm{m} \ll \kappa$), the quantum limit is $n_\mathrm{f,min}^\mathrm{q} = \kappa/(4\omega_\mathrm{m})$ for $\Delta' = -\kappa/2$. In this case, the minimum phonon number cannot reach 1, which precludes ground state cooling. In the resolved sideband limit ($\omega_\mathrm{m} \gg \kappa$), the quantum limit is simplified as $n_\mathrm{f,min}^\mathrm{q} = \kappa^2/(16\omega_\mathrm{m}^2)$ for $\Delta' = -\omega_\mathrm{m}$. In this limit, the ground state can be achieved.[158,159]

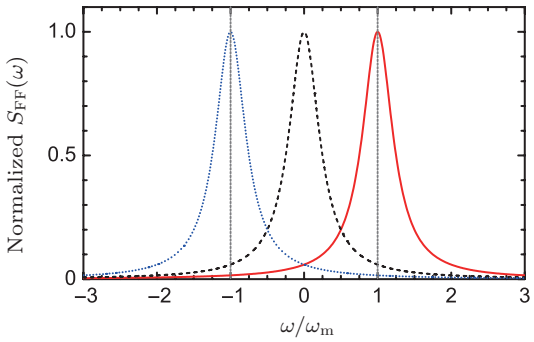


Fig. 3. Normalized optical force spectrum $S_\mathrm{FF}(\omega)$ for $\Delta' = -\omega_\mathrm{m}$ (red solid curve), 0 (black dashed curve), and ω_m (blue dotted curve). The dashed vertical lines denotes $\omega/\omega_\mathrm{m} = \pm 1$. Here, $\kappa = 0.5\omega_\mathrm{m}$.

2.3. Covariance approach

For the linear regime under strong driving, the mean phonon number can be computed exactly by employing the quantum master equation and solving a linear system of differential equations involving all the second-order moments. This approach holds for both weak and strong coupling regimes.

With the linearized Hamiltonian Eq. (17), the quantum master equation reads

$$\begin{aligned}\dot{\rho} &= \mathrm{i}[\rho, H_\mathrm{L}] + \frac{\kappa}{2}\left(2a_1\rho a_1^\dagger - a_1^\dagger a_1\rho - \rho a_1^\dagger a_1\right) \\ &\quad + \frac{\gamma}{2}(n_\mathrm{th}+1)\left(2b_1\rho b_1^\dagger - b_1^\dagger b_1\rho - \rho b_1^\dagger b_1\right) \\ &\quad + \frac{\gamma}{2}n_\mathrm{th}\left(2b_1^\dagger\rho b_1 - b_1 b_1^\dagger\rho - \rho b_1 b_1^\dagger\right). \end{aligned} \tag{33}$$

To calculate the mean phonon number, we need to determine the mean values of all the second-order moments, $\bar{N}_\mathrm{a} = \langle a_1^\dagger a_1\rangle$, $\bar{N}_\mathrm{b} = \langle b_1^\dagger b_1\rangle$, $\langle a_1^\dagger b_1\rangle$, $\langle a_1 b_1\rangle$, $\langle a_1^2\rangle$, and $\langle b_1^2\rangle$ [163,164], which are determined by a linear system of ordinary differential equations

$$\begin{aligned}\frac{\mathrm{d}}{\mathrm{d}t}\bar{N}_\mathrm{a} &= -\mathrm{i}(G\langle a_1^\dagger b_1\rangle - G^*\langle a_1^\dagger b_1\rangle^* + G\langle a_1 b_1\rangle^* \\ &\quad - G^*\langle a_1 b_1\rangle) - \kappa\bar{N}_\mathrm{a}, \end{aligned} \tag{34}$$

$$\begin{aligned}\frac{\mathrm{d}}{\mathrm{d}t}\bar{N}_\mathrm{b} &= -\mathrm{i}(-G\langle a_1^\dagger b_1\rangle + G^*\langle a_1^\dagger b_1\rangle^* + G\langle a_1 b_1\rangle^* \\ &\quad - G^*\langle a_1 b_1\rangle) - \gamma\bar{N}_\mathrm{b} + \gamma n_\mathrm{th}, \end{aligned} \tag{35}$$

$$\begin{aligned}\frac{\mathrm{d}}{\mathrm{d}t}\langle a_1^\dagger b_1\rangle &= \left[-\mathrm{i}(\Delta'+\omega_\mathrm{m}) - \frac{\kappa+\gamma}{2}\right]\langle a_1^\dagger b_1\rangle \\ &\quad - \mathrm{i}(G^*\bar{N}_\mathrm{a} - G^*\bar{N}_\mathrm{b} + G\langle a_1^2\rangle^* - G^*\langle b_1^2\rangle), \end{aligned} \tag{36}$$

$$\begin{aligned}\frac{\mathrm{d}}{\mathrm{d}t}\langle a_1 b_1\rangle &= \left[\mathrm{i}(\Delta'-\omega_\mathrm{m}) - \frac{\kappa+\gamma}{2}\right]\langle a_1 b_1\rangle \\ &\quad - \mathrm{i}(G\bar{N}_\mathrm{a} + G\bar{N}_\mathrm{b} + G + G^*\langle a_1^2\rangle + G\langle b_1^2\rangle), \end{aligned} \tag{37}$$

$$\frac{\mathrm{d}}{\mathrm{d}t}\langle a_1^2\rangle = (2\mathrm{i}\Delta' - \kappa)\langle a_1^2\rangle - 2\mathrm{i}G\left(\langle a_1 b_1\rangle + \langle a_1^\dagger b_1\rangle^*\right), \quad (38)$$

$$\frac{\mathrm{d}}{\mathrm{d}t}\langle b_1^2\rangle = (-2\mathrm{i}\omega_\mathrm{m} - \gamma)\langle b_1^2\rangle - 2\mathrm{i}(G^*\langle a_1 b_1\rangle + G\langle a_1^\dagger b_1\rangle). \quad (39)$$

Note that in the above calculation, cut-off of the density matrix is not necessary and the solutions are exact.

In the stable regime, which requires $|G|^2 < -(4\Delta'^2 + \kappa^2)\omega_\mathrm{m}/(16\Delta')$ for red detuning $\Delta' < 0$,[165] the system finally reaches the steady state, and the derivatives in the above equations all become zero. Then, the second-order moments in the steady state satisfy a set of algebraic equations. Under the condition $\Delta' = -\omega_\mathrm{m}$ and cooperativity $C \equiv 4|G|^2/(\gamma\kappa) \gg 1$, the final phonon occupancy reads[163]

$$\bar{N}_\mathrm{std} \simeq \frac{4|G|^2 + \kappa^2}{4|G|^2(\kappa+\gamma)}\gamma n_\mathrm{th} + \frac{4\omega_\mathrm{m}^2\left(\kappa^2 + 8|G|^2\right) + \kappa^2\left(\kappa^2 - 8|G|^2\right)}{16\omega_\mathrm{m}^2(4\omega_\mathrm{m}^2 + \kappa^2 - 16|G|^2)}. \quad (40)$$

Here, the first term, being proportional to the environmental thermal phonon number n_th, is the classical cooling limit; the second term, which does not depend on n_th, corresponds to the quantum cooling limit. This quantum limit originates from the quantum backaction, consisting of both dissipation quantum backaction related to the cavity dissipation and interaction quantum backaction associated with the optomechanical interaction. In the resolved sideband case, equation (40) reduces to

$$\bar{N}_\mathrm{std} \simeq \frac{\gamma(4|G|^2 + \kappa^2)}{4|G|^2(\kappa+\gamma)}n_\mathrm{th} + \frac{\kappa^2 + 8|G|^2}{16(\omega_\mathrm{m}^2 - 4|G|^2)}. \quad (41)$$

In the weak coupling regime, it further reduces to $\bar{N}_\mathrm{std}^\mathrm{wk} \simeq \gamma n_\mathrm{th}/(\Gamma+\gamma) + \kappa^2/(16\omega_\mathrm{m}^2)$ with $\Gamma = 4|G|^2/\kappa$. In the strong coupling regime, $\bar{N}_\mathrm{std}^\mathrm{str} \simeq \gamma n_\mathrm{th}/(\kappa+\gamma) + |G|^2/[2(\omega_\mathrm{m}^2 - 4|G|^2)]$. In this case, the classical limit is restricted by the cavity dissipation rate κ, while the interaction quantum backaction limit suffers from high coupling rate $|G|$.

To study the cooling dynamics beyond the steady state, the differential equations need to be solved to obtain the time evolution of the mean phonon number $\bar{N}_\mathrm{b}$. For weak coupling, we have $\bar{N}_\mathrm{b}^\mathrm{wk} \simeq n_\mathrm{th}(\gamma + \Gamma\,\mathrm{e}^{-\Gamma t})/(\gamma+\Gamma) + [\kappa^2/(16\omega_\mathrm{m}^2)](1 - \mathrm{e}^{-\Gamma t})$, which shows that the mean phonon number decays exponentially with the cooling rate Γ. This cooling rate is limited by the coupling strength, since in the cooling route $A \to E$ as shown in Fig. 2, the energy flow from the mechanical mode to the optical mode (process A) is slower than the cavity dissipation (process E).

In the strong coupling regime, the time evolution of the mean phonon number is described by[163]

$$\bar{N}_\mathrm{b}^\mathrm{str} = \bar{N}_{\mathrm{b},1}^\mathrm{str} + \bar{N}_{\mathrm{b},2}^\mathrm{str},$$
$$\bar{N}_{\mathrm{b},1}^\mathrm{str} \simeq n_\mathrm{th}\frac{\gamma + \mathrm{e}^{-(\kappa+\gamma)t/2}\left[\kappa - \gamma + (\kappa+\gamma)\cos(\omega_+ - \omega_-)t\right]/2}{\kappa+\gamma},$$
$$\bar{N}_{\mathrm{b},2}^\mathrm{str} \simeq \frac{|G|^2\left[1 - \mathrm{e}^{-(\kappa+\gamma)t/2}\cos(\omega_+ + \omega_-)t\cos(\omega_+ - \omega_-)t\right]}{2(\omega_\mathrm{m}^2 - 4|G|^2)}, \quad (42)$$

where $\omega_\pm = \sqrt{\omega_\mathrm{m}^2 \pm 2|G|\omega_\mathrm{m}}$ are the normal eigenmode frequencies. The phonon occupancy exhibits oscillation under an exponentially-decaying envelope and can be divided into two distinguishable parts $\bar{N}_{\mathrm{b},1}^\mathrm{str}$ and $\bar{N}_{\mathrm{b},2}^\mathrm{str}$, where the first part originates from energy exchange between optical and mechanical modes, and the second part is induced by quantum backaction. $\bar{N}_{\mathrm{b},1}^\mathrm{str}$ reveals Rabi oscillation with frequency $\sim 2|G|$, whereas the envelopes have the same exponential decay rate $\Gamma' = (\kappa+\gamma)/2$ regardless of the coupling strength $|G|$. This is because, in the strong coupling regime, the cooling route $A \to E$ is subjected to the cavity dissipation (process E), which has slower rate than the energy exchange between phonons and photons (process A). This saturation prevents a higher cooling speed for stronger coupling. Figures 4(a) and 4(b) plot the numerical results based on the master equation for various G. It shows that for weak coupling, the cooling rate increases rapidly as the coupling strength increases, whereas for strong coupling the envelope decay no longer increases, instead the oscillation frequency becomes larger.

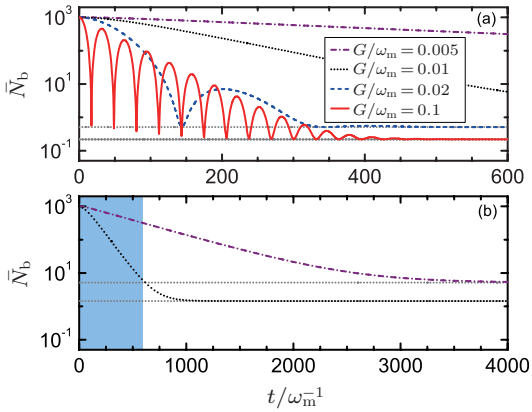


Fig. 4. (a) Time evolution of mean phonon number $\bar{N}_\mathrm{b}$ for $G/\omega_\mathrm{m} = 0.005, 0.01, 0.02$, and 0.1 (numerical results). (b) $\bar{N}_\mathrm{b}$ for $G/\omega_\mathrm{m} = 0.005$ and 0.01 with a wider time interval. The shadowed region shows the same time interval with that in panel (a). Other parameters: $n_\mathrm{th} = 10^3$, $\gamma/\omega_\mathrm{m} = 10^{-5}$, $\kappa/\omega_\mathrm{m} = 0.05$. The dotted horizontal lines correspond to the steady-state cooling limits, given by Eq. (41). Figures reproduced with permission from Ref. [163], copyright (2013) by the American Physical Society.

3. Recent experimental progresses

Pioneering work of cavity optomechanical cooling dates back to 1960th by Braginsky and coworkers,[6,7] where they

demonstrated the modification of mechanical damping rate as a result of the retarded nature of the cavity-enhanced optical force due to the finite cavity photon lifetime. In 2006, radiation pressure cooling was realized in three groups using different optomechanical systems, including suspended micromirrors[17,18] (Figs. 5(a) and 5(b)) and microtoroids.[19] Later in 2008, cooling in the resolved sideband regime was achieved.[20] Soon afterwards, with environmental pre-cooling under cryogenic condition, cooling to only a few phonons was demonstrated[21–23] (Figs. 5(c) and 5(d)). Recently, several groups have cooled the mechanical motion close to the quantum ground state both in the microwave domain[24,25] (Fig. 6) and in the optical domain[26,27,40] (Fig. 7).

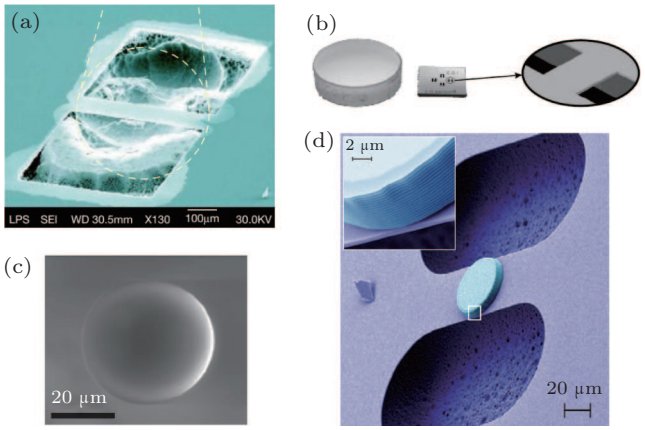


Fig. 5. (a) Scanning electron microscope (SEM) image of the cantilever, a doubly clamped free-standing Bragg mirror (520-μm long, 120-μm wide, and 2.4-μm thick) that had been fabricated by using ultraviolet excimer-laser ablation in combination with a dry-etching process. (b) Layout of the micromirror optical cavity. The microresonator mirror is etched upon a 1-cm silicon chip. The coupling mirror of the cavity is a standard low-loss silica mirror. (c) SEM image of a deformed silica microsphere. (d) SEM image of the mechanical system formed by a doubly clamped SiN beam. A circular, high-reflectivity Bragg mirror is used as the end mirror of a FP cavity. Figures reproduced with permission from: (a) Ref. [17] © 2006 Nature Publishing Group; (b) Ref. [18] © 2006 Nature Publishing Group; (c) Ref. [22] © 2009 Nature Publishing Group; (d) Ref. [21] © 2009 Nature Publishing Group.

More specifically, in Ref. [26], mean phonon occupancy down to 0.85 quanta was achieved, with the ground state occupancy probability greater than 50% ($P_g = 0.54$). In this experiment, the cavity optomechanical system consisted of a photonic crystal nanobeam resonator (Fig. 7 top panel). The carefully designed periodic patterning of the nanobeam resulted in Bragg scattering of both optical and acoustic guided waves. At the center of the nanobeam, a perturbation in the periodicity was introduced, leading to co-localized optical and mechanical resonances, which are coupled by optical gradient force. An external acoustic radiation shield consisting of a two dimensional "cross" pattern was designed to minimize the mechanical anchor damping through phononic bandgap. The optomechanical device was placed in a continuous-flow He-4 cryostat with pre-cooled environment temperature at 20 K, corresponding to about 100 initial phonon occupancy for the mechanical mode with resonance frequency as high as 3.68 GHz. The mechanical Q-factor was 10^5, corresponding to an intrinsic mechanical damping rate of 35 kHz. The optical Q-factor was 4×10^5, and thus the optical damping rate was 500 MHz. By fitting the measured data of mechanical damping effect, the single-photon optomechanical coupling strength is determined to be 910 kHz. With 2000 intracavity photons, the minimum mean phonon occupancy was observed to be 0.85 ± 0.08. The cooling was limited for higher drive powers, which resulted from the increase of the bath temperature due to optical absorption and the increase of the intrinsic mechanical damping rate induced by the generation of free carriers through optical absorption.

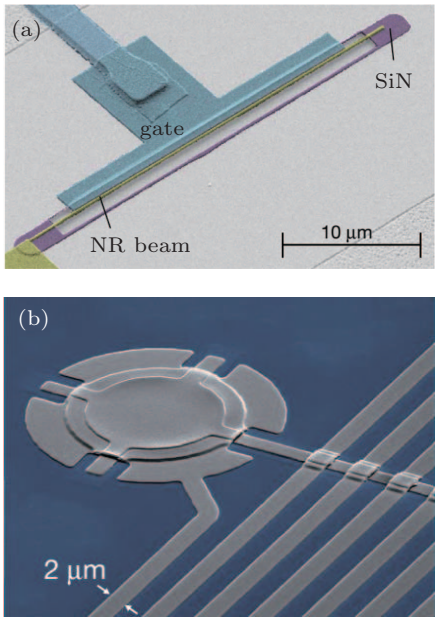


Fig. 6. (a) SEM image of the Nb-Al-SiN sample. The nanomechanical resonator is 30-μm long, 170-nm wide, and 140-nm thick, and is formed of 60 nm of stoichiometric, high-stress, low-pressure chemical-vapour-deposition SiN and 80 nm of Al. (b) SEM image of the aluminium (grey) electromechanical circuit fabricated on a sapphire (blue) substrate. A 15-μm-diameter membrane is suspended 50 nm above a lower electrode. Figures reproduced with permission from: (a) Ref. [24] © 2010 Nature Publishing Group; (b) Ref. [25] © 2011 Nature Publishing Group.

In Ref. [40], a micro-optomechanical system in the form of a spoke-supported toroidal optical microcavity (bottom panel of Fig. 7) was cooled to $n_f = 1.7$ quanta. For such microtoroidal cavity, the supported optical whispering gallery mode exhibits ultrahigh quality factor exceeding 10^8, and thus the cavity decay rate reaches $\kappa/2\pi < 10$ MHz. The mechanical resonance frequency for such spoke-anchored toroidal resonator with 31-μm diameter was 78 MHz. In a He-3 buffer gas cryostat with 650-mK temperature, the mechanical resonator was pre-cooled to ~ 200 quanta. Through optomechanical cooling, the final mean phonon occupancy was reduced to 1.7 ± 0.1. Further cooling was limited by the laser reheating of the sample and the onset of normal modes. For the latter, cooling in the strong coupling regime was limited by the

swap heating (see the next section). In this experiment, besides cooling, they also demonstrated the quantum-coherent coupling between the mechanical mode and the optical mode.

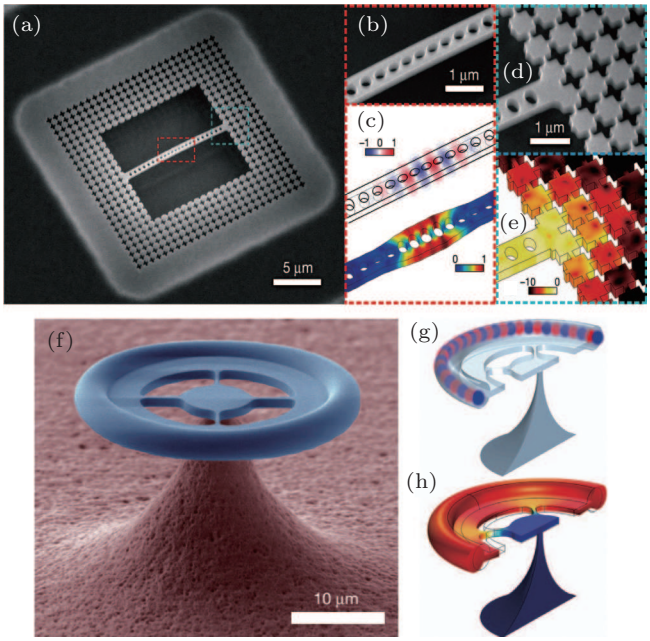


Fig. 7. Top panel: Photonic nanocrystal nanobeam cavity with phononic shield. (a) SEM image of the patterned silicon nanobeam and the external phononic bandgap shield. (b) Enlarged image of the central region of the nanobeam. (c) Simulation of the optical and mechanical modes. (d) Enlarged image of the nanobeam-shield interface. (e) Simulation of the localized acoustic resonance at the nanobeam-shield interface. Bottom panel: Spoke-supported microtoroidal cavity. (f) SEM image of the spoke-anchored toroidal resonator. (g) Sketch of an optical whispering gallery mode. (h) Simulation of the fundamental radial breathing mechanical mode. Figures reproduced with permission from: (a)–(e) Ref. [26] © 2011 Nature Publishing Group and (f)–(h) Ref. [40] © 2012 Nature Publishing Group.

4. New cooling approaches

The current cooling approach as shown in Section 2 has achieved great successes, while there are still some major challenges. First, saturation effect appears in the strong optomechanical coupling regime as a result of swap heating. Secondly, to achieve ground state cooling, it requires the resolved sideband condition, which is stringent for many cavity optomechanical systems. In this section, we review recent cooling approaches to improve the cooling performance along these directions

4.1. Cooling in the strong coupling regime

Recent experiments have reached the regime of strong optomechanical coupling, which is crucial for coherent quantum optomechanical manipulations. However, as mentioned in Section 2, strongly-coupled optomechanical cooling has predicted only limited improvement over weak coupling due to the saturation effect of the steady-state cooling rate. In Ref. [163], Liu *et al.* proposed to dynamically tailor the cooling and heating processes by exploiting the modulation of cavity dissipation. In this proposal, the internal cavity dissipation is abruptly increased each time when the Rabi oscillation reaches a minimum-phonon state. At this time the system has transited from state $|n,m\rangle$ to state $|n+1,m-1\rangle$ (Fig. 2). Once a strong dissipation pulse is applied to the cavity so that the process E dominates, the system will irreversibly transit from state $|n+1,m-1\rangle$ to state $|n,m-1\rangle$. The dissipation pulse has essentially behaves as a switch to halt the reversible Rabi oscillation, resulting in the suppression of the swap heating. Such dissipative cooling is verified in Figs. 8(a) and 8(b), which plot the modulation scheme and the corresponding time evolution of mean phonon number $\bar{N}_{\rm b}$. At the end of the first half Rabi oscillation cycle, $t \sim \pi/(2|G|)$, a dissipation pulse is applied. After that, the phonon number reaches and remains near the steady-state limit. Without modulation (blue dashed curve), the steady-state cooling limit is reached only after $t \simeq 400/\omega_{\rm m}$; while with the modulation (red solid curve), it only takes $t \simeq 8/\omega_{\rm m}$ to cool below the same limit, corresponding to 50 times faster cooling speed.

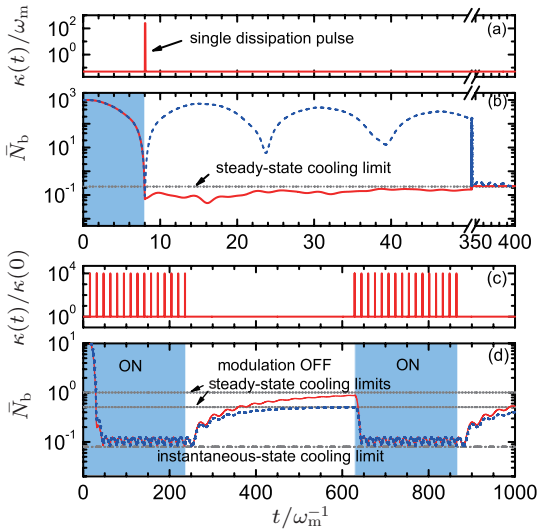


Fig. 8. (a) Modulation scheme of the cavity dissipation rate $\kappa(t)$ and (b) the corresponding time evolution of mean phonon number $\bar{N}_{\rm b}$ with (red solid curve) and without (blue dashed curve) modulation for $G/\omega_{\rm m} = 0.2$ and $\kappa/\omega_{\rm m} = 0.05$. (c) Modulation scheme of $\kappa(t)/\kappa(0)$ and (d) the corresponding $\bar{N}_{\rm b}$ for $G/\omega_{\rm m} = 0.1$, $\kappa(0)/\omega_{\rm m} = 0.01$ (red solid curve) and 0.02 (blue dashed curve). In panel (d), the two dotted horizontal lines (from top to bottom) denoting the respective steady-state cooling limits depending on the cavity decay $\kappa(0)$ given by Eq. (41); the dash-dotted line denotes the instantaneous-state cooling limit independent of $\kappa(0)$, given by Eq. (43); the "ON" and "OFF" regions corresponds that the modulation is turned on and off, respectively; the vertical coordinate range from 10 to 10^3 is not shown. Other parameters: $n_{\rm th} = 10^3$, $\gamma/\omega_{\rm m} = 10^{-5}$. Figures reproduced with permission from Ref. [163] copyright (2013) by the American Physical Society.

By periodically modulating the cavity dissipation so as to continuously suppress the swap heating, the phonon occupancy can be kept below the steady-state cooling limit. Each time after the dissipation pulse is applied, the photon number quickly drops to the vacuum state, which equivalently re-initializes the system. By periodic pulse application, the system will periodically re-initializes, which keeps the phonon occupancy in an instantaneous-state cooling limit as verified

in Figs. 8(c) and 8(d). This limit is given by [163]

$$\bar{N}_{\rm ins} \simeq \frac{\pi\gamma n_{\rm th}}{4|G|} + \frac{\pi^2|G|^4}{(\omega_{\rm m}^2-|G|^2)(\omega_{\rm m}^2-4|G|^2)}. \quad (43)$$

Here, the first term comes from $\bar{N}_{\rm b,1}^{\rm str}$ of Eq. (42) for $t \simeq \pi/(2|G|)$, which shows a $\pi\kappa/(4|G|)$ times reduction of classical steady-state cooling limit. The second term of $\sim \pi^2|G|^4/\omega_{\rm m}^4$, obtained from $\bar{N}_{\rm b,2}^{\rm str}$ when $t \simeq \pi/\omega_{\rm m}$, reveals that the second order term of $|G|/\omega_{\rm m}$ in quantum backaction has been removed, leaving only the higher-order terms. It is also demonstrated in Figs. 8(c) and 8(d) that the modulation is switchable. If the modulation is turned on ("ON" region), the system will reach the instantaneous-state cooling limit; if the modulation is turned off ("OFF" region), the system transits back to the steady-state cooling limit.

Under frequency matching condition $(\omega_+ + \omega_-)/(\omega_+ - \omega_-) = k$ $(k = 3, 5...)$ and $t \simeq \pi/(2|G|)$, the optimized instantaneous-state cooling limit is obtained as[163]

$$\bar{N}_{\rm ins}^{\rm opt} \simeq \frac{\pi\kappa}{4|G|}\left[\frac{\gamma n_{\rm th}}{\kappa} + \frac{|G|^2}{2(\omega_{\rm m}^2-4|G|^2)}\right], \quad (44)$$

which reduces both the classical and quantum steady-state cooling limits by a factor of $\pi\kappa/(4|G|)$. This reduction is significant when the system is in the deep strong coupling regime. Typically, the cooling limits can be reduced by a few orders of magnitude. For example, when $G/\omega_{\rm m} = 0.3$ and $\kappa/\omega_{\rm m} = 0.003$, it yields $\bar{N}_{\rm std} = 3.4$, while $\bar{N}_{\rm ins}^{\rm opt} = 0.03$, corresponding to more than 100 times of phonon number suppression.

4.2. Cooling beyond the resolved sideband limit

To loosen the stringent resolved sideband condition, a few approaches have been proposed, which can be divided into the following three directions: novel coupling mechanisms, parameter modulations, and hybrid systems.

4.2.1. Novel coupling mechanisms

The first direction is searching for novel optomechanical coupling mechanism, for instance, dissipative coupling, where the mechanical motion couples to the cavity decay rate instead of the cavity resonance frequency.[166] In the system described in Fig. 1, the displacement of the mechanical object couples to the cavity resonance frequency $\omega(x)$, which is sometimes termed dispersive coupling. For the dissipative coupling, the displacement of the mechanical object couples to the cavity decay rate $\kappa(x)$. It was predicted[166] that this can yield novel cooling behavior, capable of reaching the quantum ground state without the resolved sideband limit. The principle is that destructive interference effect occurs between two noise sources. In the usual dispersive coupling case, the only source of backaction force noise is the number fluctuations of the cavity field, leading to Lorentzian noise spectrum. In this dissipative coupling case, the mechanical oscillator mediates the coupling between the cavity and the cavity's dissipative bath, and there are two noise sources: one is the fluctuations of the cavity field and the other is the shot noise associated with the driving laser. Note that the latter noise process is white, and thus the interference between these two noises yields a Fano line shape for the noise spectrum. Such destructive interference allows the cavity to act as an effective zero-temperature bath at a special detuning, irrespective of the resolved sideband condition. Recent analysis shows that the quantum cooling limit of cavity optomechanical system with both dispersive and dissipative couplings can be optimized.[167]

Such dissipative coupling have been observed experimentally in a microdisk cavity coupled to a waveguide[168] (Figs. 9(a) and 9(b)) and many theoretical analysis have been performed in various systems.[169–172]

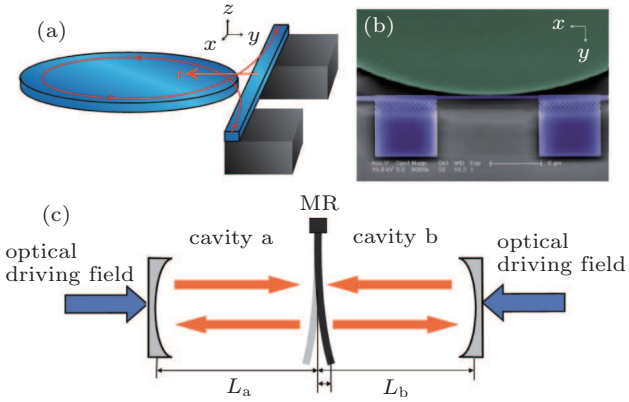


Fig. 9. (a) Schematics of the microdisk-waveguide optomechanical system for dissipative coupling. (b) SEM image of the fabricated device. (c) Schematics of the three-mirror system. The movable mirror with two perfectly reflecting surfaces is placed inside a driven cavity with two transmissive fixed mirrors. Figures reproduced with permission from: (a)–(b) Ref. [168] copyright (2009) and (c) Ref. [176] copyright (2011) by the American Physical Society.

4.2.2. Parameter modulations

The second direction is to introduce modulations of the system parameters, such as input laser intensity,[173–175] mechanical resonance frequency,[176] and other parameters[177]. In Refs. [174] and [175], optimal control method was introduced, allowing ultra-efficient cooling via pulsed laser inputs. The idea is to use interference between optical pulses incident on the system, where a sequence of fast pulses adds a term to the effective optomechanical interaction Hamiltonian. In the usual continuous driving case, the interaction term has the form $x_{\rm m}x_{\rm c}$, while the pulsed laser input generates an effective interaction term with the form $p_{\rm m}p_{\rm c}$, where $x_{\rm m}$ and $p_{\rm m}$ ($x_{\rm c}$ and $p_{\rm c}$) are the quadrature operators of the mechanical (optical) mode. By optimizing the pulse duration time, the total effective interaction is described by the beam-splitter Hamiltonian

$x_m x_c + p_m p_c \propto ab^\dagger + a^\dagger b$. As a result, the counter-rotating-wave term is eliminated, avoiding the quantum backaction heating.

In Ref. [176], Li *et al*. proposed a ground state cooling scheme by taking advantage of a mechanical resonator with a time-dependent frequency, using a three-mirror system (Fig. 9(c)). In this scheme, a strong laser input is used to generate optical spring effect, where the effective resonance frequency of the mechanical mode is determined by the optical driving. Fast ground state cooling can be achieved by designing the trajectory of the effective frequency from the initial time to the final time.

Liao and Law have investigated the cooling performance using chirped-pulse coupling by modulating the input laser intensity and phase.[178] In this scheme, owing to the frequency modulation in chirped pulses, cooling can be realized without the need for high-precision control of the laser detuning and pulse areas.

4.2.3. Hybrid systems

The third direction is to construct hybrid systems, for example, couple atoms to the optical cavity. In Ref. [179], Genes *et al*. have described a hybrid system by coupling a two-level ensemble to the cavity optomechanical system (Figs. 10(a) and 10(b)). The two-level ensemble couples to the cavity mode, creating intracavity narrow bandwidth loss or gain. It induces tailored asymmetric structure of the cavity noise spectrum interacting with the mechanical mode. As a result, This allows cooling via inhibition of the Stokes-scattering process or enhancement of anti-Stokes scattering even for low-finesse optical cavities. Ground state cooling can be realized without the requirement of resolved sideband condition, as long as the loss or gain bandwidth of the two-level ensemble is narrow enough.

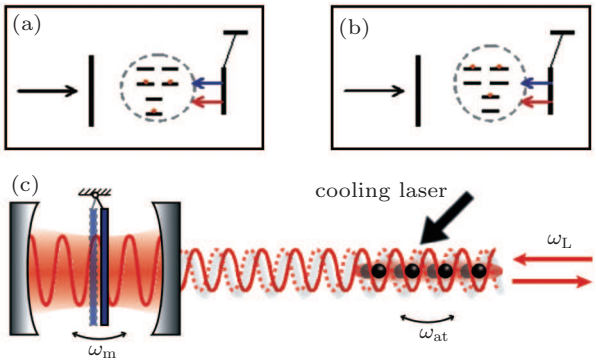


Fig. 10. (a) Couple two-level atoms to the optical cavity with a movable mirror. The atoms are in the ground states. (b) The same as (a) but the atoms are in the excited states. (c) Micromechanical membrane in a cavity coupled to a distant atomic ensemble. Figures reproduced with permission from: (a)–(b) Ref. [179] copyright (2009) and (c) Ref. [180] copyright (2013) by the American Physical Society.

A similar hybrid system containing atoms was investigated in Ref. [180] (Fig. 10(c)). Here, the atomic ensemble was trapped in an optical lattice, and the center-of-mass motion instead of internal states were considered. The cavity mode mediates the interaction between the mechanical motion of the membrane and the center-of-mass motion of the atomic ensemble, leading to the effective interaction between these two mechanical modes. By laser cooling of the atomic ensemble, the membrane motion can be cooled via the effective interaction. This does not require resolved sideband conditions for the cavity, since the cavity mode acts as an intermediary.

Before conclusion, we would like to make some remarks on the influence of laser phase noise on cavity optomechanical cooling,[181–188] which is a technical factor that limits the cooling process. The phase noise exists in many lasers, especially in diode lasers.[187] The phase fluctuation of the cooling laser will induce the photon number fluctuation in the cavity mode. This fluctuation is equivalent to a thermal bath coupled to the mechanical resonator, and thus it limits the cooling performance. In Ref. [182], Yin has proposed a double-mode cooling configuration to reduce the influence of the laser phase noise. A whispering-gallery mode cavity with double optical modes is used, and the mechanical mode is coupled to both cavity modes, with the resonance frequency equal to the frequency splitting of the two cavity modes. It is shown that the influence of phase noise can be strongly suppressed when the system is in the resolved sideband regime.

5. Summary and outlook

In summary, we have reviewed the quantum theory, recent experiments, and new directions of cavity optomechanical cooling. Particularly, we summarize the new cooling scheme along two directions: cooling in the strong coupling regime and cooling beyond the resolved sideband limit. Novel cooling schemes for efficiently suppressing the thermal noise are still being explored. These schemes add complexity to the current experimental systems, and thus efforts should be taken to demonstrate these schemes in real experiments, which would be possible in the near future. There are more appealing challenges such as cooling massive mechanical objects up to kilograms and room-temperature ground state cooling of mechanical resonators.

With currently rapid experimental and theoretical advances in cavity optomechanics, it opens up new avenues to the foundations of quantum physics and applications. Quantum manipulation of macroscopic/mesoscopic mechanical objects provides a direct method to test fundamental quantum theory in a hitherto unachieved parameter regime. For example, micro mechanical structures typically consist of 10^{14} atoms and weigh 10^{-11} kilograms, while gravitational wave detectors comprise more than 10^{20} atoms and weigh up to several kilogram. For applications, cavity optomechanics provides new aspects for measurement with high precision and

for sensing with high sensitivity. Particularly, cavity optomechanics offers a new architecture for solid-state realization of quantum information processing. The development of cavity optomechanical cooling will enable quantum manipulation of mechanical objects and generation of non-classical mechanical states, which will provide unique resources for quantum communication and quantum computation.

Acknowledgments

We thank Hu Yi-Wen and Luan Xing-Sheng for helpful discussion.

References

[1] Hänsch T W and Schawlow A L 1975 *Opt. Commun.* **13** 68
[2] Wineland D J and Dehmelt H 1975 *Bull. Am. Phys. Soc.* **20** 637
[3] Stenholm S 1986 *Rev. Mod. Phys.* **58** 699
[4] Ashkin A 1978 *Phys. Rev. Lett.* **40** 729
[5] Metzger C H and Karrai K 2004 *Nature* **432** 1002
[6] Braginsky V B and Manukin A B 1967 *Sov. Phys. JETP* **25** 653
[7] Braginsky V B, Manukin A B and Tikhonov M Y 1970 *Sov. Phys. JETP* **31** 829
[8] Dorsel A, McCullen J D, Meystre P, Vignes E and Walther H 1983 *Phys. Rev. Lett.* **51** 1550
[9] Mancini S, Vitali D and Tombesi P 1998 *Phys. Rev. Lett.* **80** 688
[10] Cohadon P F, Heidmann A and Pinard M 1999 *Phys. Rev. Lett.* **83** 3174
[11] Kleckner D and Bouwmeester D 2006 *Nature* **444** 75
[12] Corbitt T, Wipf C, Bodiya T, Ottaway D, Sigg D, Smith N, Whitcomb S and Mavalvala N 2007 *Phys. Rev. Lett.* **99** 160801
[13] Poggio M, Degen C L, Mamin H J and Rugar D 2007 *Phys. Rev. Lett.* **99** 17201
[14] Carmon T, Rokhsari H, Yang L, Kippenberg T J and Vahala K J 2005 *Phys. Rev. Lett.* **94** 223902
[15] Kippenberg T J, Rokhsari H, Carmon T, Scherer A and Vahala K J 2005 *Phys. Rev. Lett.* **95** 033901
[16] Rokhsari H, Kippenberg T J, Carmon T and Vahala K J 2005 *Opt. Express* **13** 5293
[17] Gigan S, Böhm H R, Paternostro M, Blaser F, Langer G, Hertzberg J B, Schwab K C, Bäuerle D, Aspelmeyer M and Zeilinger A 2006 *Nature* **444** 67
[18] Arcizet O, Cohadon P F, Briant T, Pinard M and Heidmann A 2006 *Nature* **444** 71
[19] Schliesser A, Del'Haye P, Nooshi N, Vahala K J and Kippenberg T J 2006 *Phys. Rev. Lett.* **97** 243905
[20] Schliesser A, Rivière R, Anetsberger G, Arcizet O and Kippenberg T J 2008 *Nat. Phys.* **4** 415
[21] Gröblacher S, Hertzberg J B, Vanner M R, Cole G D, Gigan S, Schwab K C and Aspelmeyer M 2009 *Nat. Phys.* **5** 485
[22] Park Y S and Wang H 2009 *Nat. Phys.* **5** 489
[23] Schliesser A, Arcizet O, Rivère R, Anetsberger G and Kippenberg T J 2009 *Nat. Phys.* **5** 509
[24] Rocheleau T, Ndukum T, Macklin C, Hertzberg J B, Clerk A A and Schwab K C 2010 *Nature* **463** 72
[25] Teufel J D, Donner T, Li D, Harlow J W, Allman M S, Cicak K, Sirois A J, Whittaker J D, Lehnert K W and Simmonds R W 2011 *Nature* **475** 359
[26] Chan J, Mayer A T P, Safavi-Naeini A H, Hill J T, Krause A, Gröblacher S, Aspelmeyer M and Painter O 2011 *Nature* **478** 89
[27] Riviere R, Deleglise S, Weis S, Gavartin E, Arcizet O, Schliesser A and Kippenberg T 2011 *Phys. Rev. A* **83** 063835
[28] Agarwal G S and Huang S 2010 *Phys. Rev. A* **81** 041803
[29] Weis S, Rivière R, Deléglise S, Gavartin E, Arcizet O, Schliesser A and Kippenberg T J 2010 *Science* **330** 1520
[30] Safavi-Naeini A H, Alegre T P M, Chan J, Eichenfield M, Winger M, Lin Q, Hill J T, Chang D E and Painter O 2011 *Nature* **472** 69
[31] Qu K and Agarwal G S 2013 *Phys. Rev. A* **87** 031802
[32] Karuza M, Biancofiore C, Bawaj M, Molinelli C, Galassi M, Natali R, Tombesi P, Giuseppe G D and Vitali D 2013 *Phys. Rev. A* **88** 013804
[33] Fiore V, Yang Y, Kuzyk M C, Barbour R, Tian L and Wang H 2011 *Phys. Rev. Lett.* **107** 133601
[34] Dobrindt J M, Wilson-Rae I and Kippenberg T J 2008 *Phys. Rev. Lett.* **101** 263602
[35] Gröblacher S, Hammerer K, Vanner M R and Aspelmeyer M 2009 *Nature* **460** 724
[36] Huang S and Agarwal G S 2009 *Phys. Rev. A* **80** 033807
[37] Akram U, Kiesel N, Aspelmeyer M and Milburn G J 2010 *New J. Phys.* **12** 083030
[38] Teufel J D, Li D, Allman M S, Cicak K, Sirois A J, Whittaker J D and Simmonds R W 2011 *Nature* **471** 204
[39] Chen H J and Mi X W 2011 *Chin. Phys. B* **20** 124203
[40] Verhagen E, Deléglise S, Weis S, Schliesser A and Kippenberg T J 2012 *Nature* **482** 63
[41] Palomaki T A, Harlow J W, Teufel J D, Simmonds R W and Lehnert K W 2013 *Nature* **495** 210
[42] Tian L and Wang H 2010 *Phys. Rev. A* **82** 053806
[43] Wang Y D and Clerk A A 2012 *Phys. Rev. Lett.* **108** 153603
[44] Tian L 2012 *Phys. Rev. Lett.* **108** 153604
[45] Barzanjeh S, Abdi M, Milburn G J, Tombesi P and Vitali D 2012 *Phys. Rev. Lett.* **109** 130503
[46] Hill J T, Safavi-Naeini A H, Chan J and Painter O 2012 *Nat. Commun.* **3** 1196
[47] Dong C, Fiore V, Kuzyk M C and Wang H 2012 *Science* **338** 1609
[48] Liu Y, Davanco M, Aksyuk V and Srinivasan K 2013 *Phys. Rev. Lett.* **110** 223603
[49] Tomes M and Carmon T 2009 *Phys. Rev. Lett.* **102** 113601
[50] Ma R, Schliesser A, Del'Haye P, Dabirian A, Anetsberger G and Kippenberg T J 2007 *Opt. Lett.* **32** 2200
[51] Jiang X, Lin Q, Rosenberg J, Vahala K and Painter O 2009 *Opt. Express* **17** 20911
[52] Wiederhecker G S, Chen L, Gondarenko A and Lipson M 2009 *Nature* **462** 633
[53] Eichenfield M, Camacho R, Chan J, Vahala K J and Painter O 2009 *Nature* **459** 550
[54] Eichenfield M, Chan J, Camacho R M, Vahala K J and Painter O 2009 *Nature* **462** 78
[55] Li Y, Zheng J, Gao J, Shu J, Aras M S and Wong C W 2010 *Opt. Express* **18** 23844
[56] Zheng J, Li Y, Aras M S, Stein A, Shepard K L and Wong C W 2012 *App. Phys. Lett.* **100** 211908
[57] Thompson J D, Zwickl B M, Jayich A M, Marquardt F, Girvin S M and Harris J G E 2008 *Nature* **452** 72
[58] Cheung H K and Law C K 2011 *Phys. Rev. A* **84** 023812
[59] Bui C H, Zheng J, Hoch S W, Lee L Y T, Harris J G E and Wong C W 2012 *App. Phys. Lett.* **100** 021110
[60] Li H K, Liu Y C, Yi X, Zou C L, Ren X X and Xiao Y F 2012 *Phys. Rev. A* **85** 053832
[61] Anetsberger G, Arcizet O, Unterreithmeier Q P, Rivière R, Schliesser A, Weig E M, Kotthaus J P and Kippenberg T J 2009 *Nat. Phys.* **5** 909
[62] Li M, Pernice W H P, Xiong C, Baehr-Jones T, Hochberg M and Tang H X 2008 *Nature* **456** 480
[63] Favero I, Stapfner S, Hunger D, Paulitschke P, Reichel J, Lorenz H, Weig E M and Karrai K 2009 *Opt. Express* **17** 12813
[64] Zheng J, Sun X, Li Y, Poot M, Dadgar A, Shi N, Pernice W H P, Tang H X and Wong C W 2012 *Opt. Express* **20** 26486
[65] Hu Y W, Li B B, Liu Y X, Xiao Y F and Gong Q 2013 *Opt. Commun.* **291** 380
[66] Chang D E, Regal C A, Papp S B, Wilson D J, Painter O, Kimble H J and Zoller P 2010 *Proc. Natl. Acad. Sci. USA* **107** 1005
[67] Romero-Isart O, Juan M L, Quidant R and Cirac J I 2010 *New J. Phys.* **12** 033015
[68] Li T, Kheifets S and Raizen M G 2011 *Nat. Phys.* **7** 527
[69] Gieseler J, Deutsch B, Quidant R and Novotny L 2012 *Phys. Rev. Lett.* **109** 103603

[70] Pender G A T, Barker P F, Marquardt F, Millen J and Monteiro T S 2012 *Phys. Rev. A* **85** 021802

[71] Yin Z Q, Li T and Feng M 2011 *Phys. Rev. A* **83** 013816

[72] Yin Z Q, Li T, Zhang X and Duan L M 2013 arXiv: 1305.1701

[73] Brennecke F, Ritter S, Donner T and Esslinger T 2008 *Science* **322** 235

[74] Murch K W, Moore K L, Gupta S and Stamper-Kurn D M 2008 *Nat. Phys.* **4** 561

[75] Zhang K, Meystre P and Zhang W 2012 *Phys. Rev. Lett.* **108** 240405

[76] Regal C A, Teufel J D and Lehnert K W 2008 *Nat. Phys.* **4** 555

[77] Rabl P 2011 *Phys. Rev. Lett.* **107** 063601

[78] Nunnenkamp A, Børkje K and Girvin S M 2011 *Phys. Rev. Lett.* **107** 063602

[79] Nunnenkamp A, Børkje K and Girvin S M 2012 *Phys. Rev. A* **85** 051803

[80] Ludwig M, Safavi-Naeini A H, Painter O and Marquardt F 2012 *Phys. Rev. Lett.* **109** 063601

[81] Stannigel K, Komar P, Habraken S J M, Bennett S D, Lukin M D, Zoller P and Rabl P 2012 *Phys. Rev. Lett.* **109** 013603

[82] Xu X W, Li Y J and Liu Y X 2013 *Phys. Rev. A* **87** 025803

[83] Liao J Q, Cheung H K and Law C K 2012 *Phys. Rev. A* **85** 025803

[84] Ren X X, Li H K, Yan M Y, Liu Y C, Xiao Y F and Gong Q 2013 *Phys. Rev. A* **87** 033807

[85] Liao J Q and Law C K 2013 *Phys. Rev. A* **87** 043809

[86] Jia W Z and Wang Z D 2013 arXiv: 1308.1339

[87] Lemonde M A, Didier N and Clerk A A 2013 *Phys. Rev. Lett.* **111** 053602

[88] Børkje K, Nunnenkamp A, Teufel J D and Girvin S M 2013 *Phys. Rev. Lett.* **111** 053603

[89] Liu Y C, Xiao Y F, Chen Y L, Yu X C and Gong Q 2013 *Phys. Rev. Lett.* **111** 083601

[90] Kronwald A and Marquardt F 2013 *Phys. Rev. Lett.* **111** 133601

[91] Bhattacharya M, Uys H and Meystre P 2008 *Phys. Rev. A* **77** 033819

[92] Sankey J C, Yang C, Zwickl B M, Jayich A M and Harris J G E 2010 *Nat. Phys.* **6** 707

[93] Clerk A A, Marquardt F and Harris J G E 2010 *Phys. Rev. Lett.* **104** 213603

[94] Nunnenkamp A, Børkje K, Harris J G E and Girvin S M 2010 *Phys. Rev. A* **82** 021806

[95] Vanner M R 2011 *Phys. Rev. X* **1** 021011

[96] Buchmann L F, Zhang L, Chiruvelli A and Meystre P 2012 *Phys. Rev. Lett.* **108** 210403

[97] Deng Z J, Li Y, Gao M and Wu C W 2012 *Phys. Rev. A* **85** 025804

[98] Liao J Q and Nori F 2013 *Phys. Rev. A* **88** 023853

[99] Romero-Isart O, Pflanzer A C, Blaser F, Kaltenbaek R, Kiesel N, Aspelmeyer M and Cirac J I 2011 *Phys. Rev. Lett.* **107** 020405

[100] Romero-Isart O 2011 *Phys. Rev. A* **84** 052121

[101] Pepper B, Ghobadi R, Jeffrey E, Simon C and Bouwmeester C 2012 *Phys. Rev. Lett.* **109** 023601

[102] Vitali D, Gigan S, Ferreira A, Böhm H R, Tombesi P, Guerreiro A, Vedral V, Zeilinger A and Aspelmeyer M 2007 *Phys. Rev. Lett.* **98** 030405

[103] Yin Z Q and Han Y J 2009 *Phys. Rev. A* **79** 024301

[104] Zou C L, Zou X B, Sun F W, Han Z F and Guo G C 2011 *Phys. Rev. A* **84** 032317

[105] Joshi C, Larson J, Jonson M, Andersson E and Öhberg P 2012 *Phys. Rev. A* **85** 033805

[106] Akram U, Munro W, Nemoto K and Milburn G J 2012 *Phys. Rev. A* **86** 042306

[107] Tian L 2013 *Phys. Rev. Lett.* **110** 233602

[108] Wang Y D and Clerk A A 2013 *Phys. Rev. Lett.* **110** 253601

[109] Xu X W, Zhao Y J and Liu Y X 2013 *Phys. Rev. A* **88** 022325

[110] Li H K, Ren X X, Liu Y C and Xiao Y F 2013 arXiv:1306.1035

[111] Mi X W, Bai J X, Li D J 2012 *Chin. Phys. B* **21** 030303

[112] Ma Y H and Zhou L 2013 *Chin. Phys. B* **22** 024204

[113] Zhang D, Zhang X P and Zheng Q 2013 *Chin. Phys. B* **22** 064206

[114] Jähne K, Genes C, Hammerer K, Wallquist M, Polzik E S and Zoller P 2009 *Phys. Rev. A* **79** 063819

[115] Seok H, Buchmann L F, Singh S, Steinke S K and Meystre P 2012 *Phys. Rev. A* **85** 033822

[116] Brooks D W C, Botter T, Schreppler S, Purdy T P, Brahms N and Stamper-Kurn D M 2012 *Nature* **488** 476

[117] Safavi-Naeini A H, Gröblacher S, Hill J T, Chan J, Aspelmeyer M and Painter O 2013 *Nature* **500** 185

[118] Purdy T P, Yu P L, Peterson R W, Kampel N S and Regal C A 2013 *Phys. Rev. X* **3** 031012

[119] Blencowe M P 2013 *Phys. Rev. Lett.* **111** 021302

[120] Ludwig M and Marquardt F 2013 *Phys. Rev. Lett.* **111** 073603

[121] Schmidt M, Ludwig M and Marquardt F 2012 *New J. Phys.* **14** 125005

[122] Hammerer K, Wallquist M, Genes C, Ludwig M, Marquardt F, Treutlein P, Zoller P, Ye J and Kimble H J 2009 *Phys. Rev. Lett.* **103** 063005

[123] Wallquist M, Hammerer K, Zoller P, Genes C, Ludwig M, Marquardt F, Treutlein P, Ye J and Kimble H J 2010 *Phys. Rev. A* **81** 023816

[124] Stannigel K, Rabl P, Sørensen A S, Zoller P and Lukin M D 2010 *Phys. Rev. Lett.* **105** 220501

[125] Stannigel K, Rabl P, Sørensen A S, Lukin M D and Zoller P 2011 *Phys. Rev. A* **84** 042341

[126] Habraken S J M, Stannigel K, Lukin M D, Zoller P and Rabl P 2012 *New J. Phys.* **14** 115004

[127] Bahl G, Tomes M, Marquardt F and Carmon T 2012 *Nat. Phys.* **8** 203

[128] Bahl G, Kim K H, Lee W, Liu J, Fan X and Carmon T 2013 *Nat. Commun.* **4** 1994

[129] LaHaye M D, Buu O, Camarota B and Schwab K C 2004 *Science* **304** 74

[130] Teufel J D, Donner R, Castellanos-Beltran M A, Harlow J W and Lehnert K W 2009 *Nat. Nanotech.* **4** 820

[131] Krause A G, Winger M, Blasius T D, Lin Q and Painter O 2012 *Nat. Photon.* **6** 768

[132] Forstner S, Prams S, Knittel J, van Ooijen E D, Swaim J D, Harris G I, Szorkovszky A, Bowen W P and Rubinsztein-Dunlop H 2012 *Phys. Rev. Lett.* **108** 120801

[133] Purdy T P, Peterson R W and Regal C A 2013 *Science* **339** 801

[134] Huang P, Wang P, Zhou J, Wang Z, Ju C, Wang Z, Shen Y, Duan C and Du J 2013 *Phys. Rev. Lett.* **110** 227202

[135] Kippenberg T J and Vahala K J 2007 *Opt. Express* **15** 17172

[136] Kippenberg T J and Vahala K J 2008 *Science* **321** 1172

[137] Marquardt F, Clerk A A and Girvin S M 2008 *J. Mod. Opt.* **55** 3329

[138] Genes C, Mari A, Vitali D and Tombesi P 2009 *Adv. At. Mol. Opt. Phys.* **57** 33

[139] Marquardt F and Girvin S M 2009 *Physics* **2** 40

[140] Favero I and Karrai K 2009 *Nat. Photon.* **3** 201

[141] van Thourhout D and Roels J 2010 *Nat. Photon.* **4** 211

[142] Schliesser A and Kippenberg T J 2010 *Adv. At. Mol. Opt. Phys.* **58** 207

[143] Aspelmeyer M, Gröblacher S, Hammerer K and Kiesel N 2010 *J. Opt. Soc. Am. B* **27** A189

[144] Zhang K Y, Zhou L, Dong G J and Zhang W P 2011 *Front. Phys.* **6** 237

[145] Milburn G J and Woolley M J 2011 *Acta Physica Slovaca* **61** 483

[146] Muschik C A, Krauter H, Hammerer K and Polzik E S 2011 *Quantum Inf. Proc.* **10** 839

[147] Regal C A and Lehnert K W 2011 *J. Phys. Conf. Ser.* **264** 012025

[148] Ma J and Povinelli M L 2012 *Curr. Opin. Solid State Mat. Sci.* **16** 82

[149] Stamper-Kurn D M 2012 arXiv:1204.4351

[150] Poot M and van der Zant H S J 2012 *Phys. Rep.* **511** 273

[151] Aspelmeyer M, Meystre P and Schwab K 2012 *Phys. Today* **65** 29

[152] Meystre P 2013 *Ann. Phys.* **525** 215

[153] Chen Y 2013 *J. Phys. B: At. Mol. Opt. Phys.* **46** 104001

[154] Li J J and Zhu K D 2013 *Phys. Rep.* **525** 223

[155] Aspelmeyer M, Kippenberg T J and Marquardt F 2013 arXiv:1303.0733

[156] Hu Y W, Xiao Y F, Liu Y C and Gong Q 2013 *Front. Phys.* **8** 475

[157] Yin Z Q, Geraci A A and Li T 2013 *Int. J. Mod. Phys. B* **27** 1330018

[158] Wilson-Rae I, Nooshi N, Zwerger W and Kippenberg T J 2007 *Phys. Rev. Lett.* **99** 093901

[159] Marquardt F, Chen J P, Clerk A A and Girvin S M 2007 *Phys. Rev. Lett.* **99** 093902

[160] Genes C, Vitali D, Tombesi P, Gigan S and Aspelmeyer M 2008 *Phys. Rev. A* **77** 033804
[161] Law C K 1995 *Phys. Rev. A* **51** 2537
[162] Abdi M and Bahrampour A R 2012 *Phys. Rev. A* **85** 063839
[163] Liu Y C, Xiao Y F, Luan X and Wong C W 2013 *Phys. Rev. Lett.* **110** 153606
[164] Wilson-Rae I, Nooshi N, Dobrindt J, Kippenberg T J and Zwerger W 2008 *New. J. Phys.* **10** 095007
[165] DeJesus E X and Kaufman C 1987 *Phys. Rev. A* **35** 5288
[166] Elste F, Girvin S M and Clerk A A 2009 *Phys. Rev. Lett.* **102** 207209
[167] Weiss T and Nunnenkamp A 2013 *Phys. Rev. A* **88** 023850
[168] Li M, Pernice W H P and Tang H X 2009 *Phys. Rev. Lett.* **103** 223901
[169] Xuereb A, Schnabel R and Hammerer K 2011 *Phys. Rev. Lett.* **107** 213604
[170] Weiss T, Bruder C and Nunnenkamp A 2013 *New J. Phys.* **15** 045017
[171] Yan M Y, Li H K, Liu Y C, Jin W L and Xiao Y F 2013 *Phys. Rev. A* **88** 023802
[172] Gu W J, Li G X and Yang Y P 2013 *Phys. Rev. A* **88** 013835
[173] Vanner M R, Pikovski I, Cole G D, Kim M S, Brukner C, Hammerer K, Milburn G J and Aspelmeyer M 2011 *Proc. Natl. Acad. Sci. USA* **108** 16182
[174] Wang X, Vinjanampathy S, Strauch F W and Jacobs K 2011 *Phys. Rev. Lett.* **107** 177204
[175] Machnes S, Cerrillo J, Aspelmeyer M, Wieczorek W, Plenio M B and Retzker A 2012 *Phys. Rev. Lett.* **108** 153601
[176] Li Y, Wu L A and Wang Z D 2011 *Phys. Rev. A* **83** 043804
[177] Farace A and Giovannetti V 2012 *Phys. Rev. A* **86** 013820
[178] Liao J Q and Law C K 2011 *Phys. Rev. A* **84** 053838
[179] Genes C, Ritsch H and Vitali D 2009 *Phys. Rev. A* **80** 061803
[180] Vogell B, Stannigel K, Zoller P, Hammerer K, Rakher M T, Korppi M, Jöckel A and Treutlein P 2013 *Phys. Rev. A* **87** 023816
[181] Diósi L 2008 *Phys. Rev. A* **78** 021801
[182] Yin Z Q 2009 *Phys. Rev. A* **80** 033821
[183] Rabl P, Genes C, Hammerer K and Aspelmeyer M 2009 *Phys. Rev. A* **80** 063819
[184] Phelps G A and Meystre P 2011 *Phys. Rev. A* **83** 063838
[185] Abdi M, Barzanjeh S, Tombesi P and Vitali D 2011 *Phys. Rev. A* **84** 032325
[186] Ghobadi R, Bahrampour A R and Simon C 2011 *Phys. Rev. A* **84** 063827
[187] Kippenberg T J, Schliesser A and Gorodetsky M 2013 *New J. Phys.* **15** 015019
[188] Zhang D and Zheng Q 2013 *Chin. Phys. Lett.* **30** 024213